

# Electrochemical studies on sulfonephthaleins. Part 2.<sup>1</sup>

## Electrochemical reduction mechanism of catechol violet in aqueous solutions on a mercury electrode

Refat Abdel-Hamid

Department of Chemistry, Faculty of Science, Sohag, Egypt

The electrochemical reduction mechanism of catechol violet at a hanging mercury electrode, HMDE, in aqueous buffer solutions of different pHs has been studied in detail by cyclic voltammetry, double potential step chronoamperometry, chronocoulometry and digital simulation. Catechol violet shows at lower pHs (< 7) a single diffusion-controlled two-electron wave while at higher pHs (> 8), two diffusion-controlled mono-electron waves are given. It is concluded that at lower pHs the reduction pathway follows an ECEC, first-order mechanism in which E represents a reversible electron transfer and C is an irreversible protonation reaction. The rate-determining step is the protonation of the monoanion formed after the second electron transfer. At higher pHs, the reduction proceeds *via* two steps, an irreversible electron transfer followed by an EC, first-order process. The homogeneous parameters were measured by comparing the experimental chronocoulometric data with the theoretical working curves. The heterogeneous parameters were obtained by comparing the experimental cyclic voltammetric responses with the digital simulated results.

Electrochemistry of phenolsulfonephthaleins has been investigated in a few instances.<sup>2-6</sup> Literature concerning the electrochemical reduction of catechol violet is quite scarce<sup>1</sup> and the electroreduction mechanism of catechol violet appears to be incompletely understood. Since it is used in spectrophotometric trace measurements of metal ions,<sup>7</sup> as a metallochromic indicator,<sup>8-11</sup> in flow injection spectrophotometry for trace elements in environmental<sup>12-14</sup> and food<sup>15</sup> analyses, in the stripping voltammetric trace analysis of titanium<sup>16</sup> as well as for application as a charge-transfer mediator in the oxidation of nicotinamide adenine dinucleotide (NADH)<sup>17</sup> we have investigated the mechanism of its electrochemical reduction.

The purpose of the investigation was to carry out a quantitative detailed study of the electrochemical reduction of catechol violet, pyrocatechol sulfonephthalein,† in aqueous buffer solutions at different pHs. Various electrochemical techniques were used: cyclic voltammetry using the diagnostic criteria derived by Nicholson and Shain for various electrode mechanisms,<sup>18-20</sup> controlled potential coulometry, digital simulation developed by Feldberg<sup>21</sup> which provides a powerful independent route in the interpretation of cyclic voltammograms by comparison of the experimental and simulated results and double step chronoamperometry and chronocoulometry, which are more powerful for quantitative characterization of complex electrode processes.

### Experimental

All measurements were made at 298 K. Electrochemical experiments were carried out on an EG&G PAR Potentiostat/Galvanostat model 363A. An EG&G three elements electrolysis cell system model SMDE 303A was used. A hanging mercury electrode, HMDE, in the small hanging drop mode was used as the working electrode to reduce the non-Faradaic current relative to the Faradaic one.<sup>22</sup> The electrode area is  $4.83 \times 10^{-2}$  cm<sup>2</sup>. Platinum wire and silver/silver chloride aqueous potassium chloride electrodes were used as counter and reference electrodes, respectively. The electrochemical system

was interfaced with an IBM Value Point 433 DX/DP Computer. The data were captured, stored and manipulated with EG&G M270/500 software. Positive feedback was used for compensation of the solution resistance. All solutions were freshly prepared and kept in an inert nitrogen atmosphere. Solutions were purged with pure nitrogen before measurements were taken and an atmosphere of nitrogen was maintained above the working solution. The cyclic voltammograms and chronoamperograms were recorded with equally spaced time per point, both for the pure supporting electrolyte solution and in the presence of the substrate. The background data were subtracted digitally implying the assumption of a simple additivity of Faradaic and non-Faradaic currents minimizing effects such as double layer charging currents. The reaction parameters were determined (or confirmed) by analysing the cyclic voltammetric responses using the simulation CVSIM and CVFIT softwares.<sup>23</sup>

The CVSIM and CVFIT programs include corrections of *iR* drop in the cyclic voltammograms. For this correction, the uncompensated resistance was analysed by potential step chronoamperometry. The initial potential was set to the same potential as the initial potential in the cyclic voltammetric experiments and then a step of  $-50$  mV to the initial potential was applied for 1 or 2 ms. Since the procedure did not involve Faradaic current, the current response follows eqn. (1) where *i*,

$$i_t = \frac{\Delta E}{R} \exp\left(\frac{-t}{RC_{dl}}\right) \quad (1)$$

is the response current at time *t* and  $\Delta E$  is the potential step applied. On plotting  $\ln(i_t)$  vs. *t*, the uncompensated resistance *R* is obtained from the intercept.<sup>24</sup>

Controlled potential coulometric experiments were performed with an EG&G PAR model 377 Coulometric Cell system. All controlled potential coulometric experiments were carried out at potentials determined by cyclic voltammograms.

### Results and discussion

According to Wakley and Varga,<sup>7</sup> catechol violet molecule provides four species. The neutral H<sub>4</sub>CV form was detected

† IUPAC preferred name is 2-[(3,4-dihydroxyphenyl)(3-hydroxy-4-oxocyclohexa-2,5-dienylidene)methyl]benzenesulfonate.

**Table 1** Cyclic voltammetric data for 1.0 mmol dm<sup>-3</sup> catechol violet at different pHs at  $\nu = 0.2 \text{ V s}^{-1}$ 

pH	$-E_p/\text{V}$	$i_p/\mu\text{A}$	pH	$-E_p/\text{V}$	$i_p/\mu\text{A}$	2nd wave	
						$-E_p/\text{V}$	$i_p/\mu\text{A}$
1.68	0.467	1.758	6.76	0.761	2.697	—	—
1.94	0.476	2.728	8.40	0.740	2.169	0.810	1.57
2.47	0.505	2.753	9.45	0.724	0.178	0.856	1.65
4.23	0.613	2.918	10.94	0.726	0.636	0.917	2.879
5.44	0.682	3.257					

in highly acidic solutions. Between pH 1 and 2, the sulfonic acid group dissociates forming the  $\text{H}_3\text{CV}^-$  species ( $\text{H}_4\text{CV} \rightleftharpoons \text{H}_3\text{CV}^- + \text{H}^+$ ,  $\text{p}K_1 = 0.26$ ). In the pH range 5–7, the  $\text{H}_2\text{CV}^{2-}$  species was detected owing to the dissociation of a hydroxy group ( $\text{H}_3\text{CV}^- \rightleftharpoons \text{H}_2\text{CV}^{2-} + \text{H}^+$ ,  $\text{p}K_2 = 7.51$ ). Finally, at higher pHs ( $> 8$ ), further hydroxy groups dissociate to form the  $\text{HCV}^{3-}$  form ( $\text{H}_2\text{CV}^{2-} \rightleftharpoons \text{HCV}^{3-} + \text{H}^+$ ,  $\text{p}K_3 = 8.33$ ). The equilibrium concentration of these species has been calculated<sup>25</sup> in the entire pH range (1.68–10.94) from the knowledge of the analytical concentration,  $\text{p}K_2$  and  $\text{p}K_3$  values of catechol violet along with the pH of the experimental solution. It was revealed that in the pH range of 1.68–5.44, the  $\text{H}_3\text{CV}^-$  form predominates, the  $\text{H}_2\text{CV}^{2-}$  species was the predominant form in the pH range of 7–8 and at higher pHs ( $> 8$ ) the  $\text{HCV}^{3-}$  form dominates.

#### Cyclic voltammetry

Cyclic voltammograms of  $1.0 \times 10^{-3} \text{ mol dm}^{-3}$  catechol violet are recorded in Britton–Robinson aqueous buffer solutions over a pH range 1.68–10.9 with HMDE versus  $\text{Ag}/\text{Ag}^+$ . Generally, at  $\text{pH} < 7$ , the cyclic voltammograms exhibit a cyclic voltammetric (cv) wave corresponding to two electrons. At a constant scan rate,  $0.2 \text{ V s}^{-1}$ , the peak potential of the cv wave shifts cathodically as the pH of the solution increases thereby indicating the involvement of hydrogen ions in the reduction process. From the data cited in Table 1, one can see that in the range  $\text{pH} 1.68\text{--}6.8$ , the peak potential,  $E_p$ , correlates with the pH of the solution. The linear least-square relation obtained can be represented by eqn. (2). The number of protons

$$E_p = -0.36 - 0.059 \text{ pH} \quad r = 0.999 \quad (2)$$

consumed is calculated to be two protons in this pH range. On increasing the pH of the medium ( $\text{pH} > 7$ ), the single cv wave splits into two daughter waves in which the first one is ill defined. At higher pHs ( $\text{pH} 10.9$ ) the cyclic voltammogram exhibits two defined cv waves both corresponding to a one electron process. It is evident that the first cv wave at  $\text{pH} > 7$  is independent of pH (*cf.* Table 1), revealing that no protons are consumed during the reduction along the first cv wave. On the other hand, the peak potential for the second cv wave shifts toward more negative values on increasing the pH of the solution revealing the consumption of hydrogen ions. On plotting the peak potential versus pH, a linear relationship is obtained. The linear least-squares relation is represented in eqn. (3). The number of protons involved is estimated to be one in the pH range 8.4–10.9.

$$E_p = -0.46 - 0.042 \text{ pH} \quad r = 0.999 \quad (3)$$

**Behaviour at pH 1.8.** At pH 1.8, catechol violet gives a single cv wave (*cf.* Fig. 1). It is revealed from the results that the peak current,  $i_p$ , has a linear dependence on the square root of scan rate,  $\nu^{1/2}$ . A straight line is obtained for the relation of  $i_p$  vs.  $\nu^{1/2}$  with a correlation coefficient of 0.999. Thus, the electrochemical reduction process is diffusion-controlled in nature. The peak current ratio,  $i_p^a/i_p^c$ , estimated from eqn. (4),

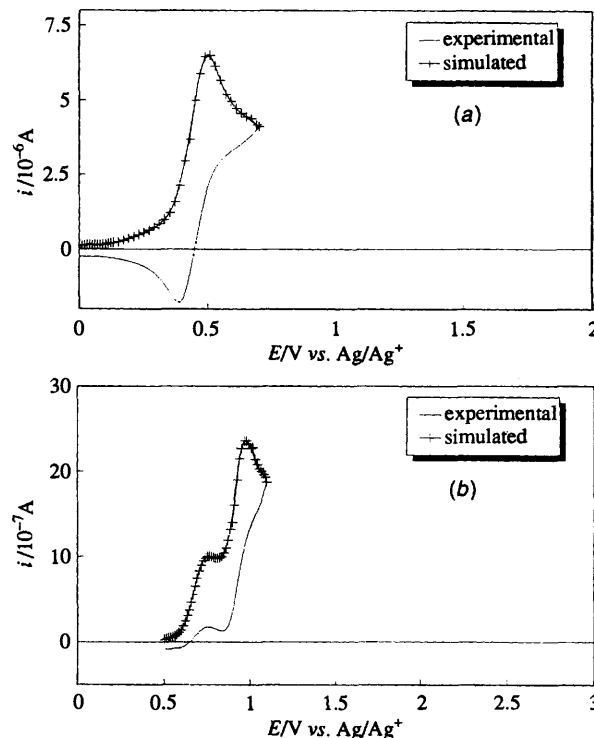


**Fig. 1** Best fit of the cyclic experimental and simulated voltammograms for the possible reduction mechanisms of catechol violet: (a) pH 1.8, (b) pH 10.94

increases with increasing scan rate from 0.59 at  $0.1 \text{ V s}^{-1}$  to 0.79 at  $10.0 \text{ V s}^{-1}$ . In eqn. (4)  $i_p^a(0)$  is the uncorrected anodic peak

$$\frac{i_p^a}{i_p^c} = \frac{i_p^a(0)}{i_p^c} + \frac{0.485 \times i_\lambda(0)}{i_p^c} + 0.086 \quad (4)$$

current and  $i_\lambda(0)$  is the uncorrected current at the switching potential  $E_\lambda$ , both measured with respect to the zero current base line.<sup>18</sup> Furthermore, the current function,  $i_p^c/\nu^{1/2}$ , decreases from 9.08 to 7.51 on increasing the scan rate from 0.1 to  $10.0 \text{ V s}^{-1}$ . The difference between the cathodic peak potential and the half-peak potential,  $E_p - E_{p/2}$  (73 mV at  $0.2 \text{ V s}^{-1}$ ), and the separation between anodic and cathodic peak potentials,  $\Delta E_p$  (103 mV at  $0.2 \text{ V s}^{-1}$ ), are significantly larger than the values pertaining to the normal two-electron reversible processes and they increase as the rate of the potential scan increases. Since the complete reduction of phenolsulfonephthaleins requires the transfer of two electrons,<sup>2,3</sup> also as indicated by the controlled potential coulometric results, the observed cv wave involves two electrons. Accordingly, these findings are consistent with the initial hypothesis that the electroreduction of catechol violet at lower pHs proceeds via an ECE-disproportionation (DISP) mechanism in which the radical anion resulting from the first electron addition is involved in a chemical step yielding a species more reducible than the starting material. The broadening of the cv wave is

explained on the basis that the standard potential for the introduction of the second electron,  $E_2^\circ$ , is equal or more positive than the standard potential for the introduction of the first electron,  $E_1^\circ$ . When the difference is less than 100 mV, broader peaks with larger peak potential separation are obtained.<sup>18</sup>

A linear relation is barely reached, on plotting the peak potential as a function of scan rate, presumably owing to slow protonation of the electrogenerated radical anion. The slope of the linear portion of the plot is 26.1 mV dec<sup>-1</sup>. This points towards the ECE mechanism.

**Behaviour at pH 10.94.** At pH 10.94, the voltammetric wave of catechol violet splits into two monoelectronic cathodic waves (cf. Fig. 1). At a given concentration of the depolarizer (1.0 mmol dm<sup>-3</sup>), the first wave becomes ill defined, while the height of the second wave increases on increasing the scan rate. It is found that the peak current for the second wave correlates with the square root of the scan rate,  $v^{1/2}$  ( $r = 0.999$ ). On reversing the potential scan beyond the second wave to the initial potential, an anodic wave corresponding to the second wave appears in the reverse sweep of the cyclic voltammogram.

For the first wave, it seems to be irreversible, since its anodic counterpart is lacking. This suggests that the first cv wave is due to an irreversible electron transfer or reversible electron transfer coupled to an irreversible follow-up chemical reaction. Since it is pH independent, one concludes that the first cv wave is attributed to an irreversible electron transfer process. For the second cv wave, it is revealed that the cathodic and anodic peak potential separation is higher than the theoretical value for the one-electron reversible process. Moreover, the anodic to cathodic current ratio,  $i_p^a/i_p^c$ , is close to unity at all the scan rates used,  $1.03 \pm 0.03$ . The current function,  $i_p^c/v^{1/2}$ , slightly increases and the peak potential shifts cathodically by 34.9 mV dec<sup>-1</sup> with increasing scan rate. These results reveal that the second wave follows a reversible electron transfer followed by a reversible chemical reaction pathway.

#### Chronoamperometry and chronocoulometry

Although cyclic voltammetry is used in qualitative measurements, the complex nature of the electrode mechanisms limits its use in quantitative studies of coupled chemical reactions. In comparison, the potential step methods, chronoamperometry and chronocoulometry, are more suitable for such quantitative studies. In the potential step the electrochemical responses are represented by eqns. (5)–(8) where  $i(t)$  is the current at time  $t$ ,  $Q$

$$i(t < \tau) = \frac{nFAD^{1/2} C^*}{(\tau t)^{1/2}} \quad (5)$$

$$i(t > \tau) = -\frac{nFAD^{1/2} C^*}{\pi^{1/2}} \left[ \frac{1}{(t - \tau)^{1/2}} - \frac{1}{t^{1/2}} \right] \quad (6)$$

$$Q(t < \tau) = \frac{2nFAD^{1/2} C^*}{\pi^{1/2}} t^{1/2} \quad (7)$$

$$Q(t > \tau) = \frac{2nFAD^{1/2} C^*}{\pi^{1/2}} [t^{1/2} - (t - \tau)^{1/2}] \quad (8)$$

is the amount of charge that has passed at time  $t$  since the application of the potential step,  $C^*$  and  $D$  are the concentration and diffusion coefficient of the reactant, respectively, and  $A$  is the surface electrode area. In chronocoulometry, the charge ratio [eqn. (9)] is obtained from the ratio of eqn. (7) at  $t = \tau$  and eqn. (8) at  $t = 2\tau$ .

$$Q_R = \frac{Q_b}{Q_f} = \left[ \frac{Q(\tau) - Q(2\tau)}{Q(\tau)} \right] \quad (9)$$

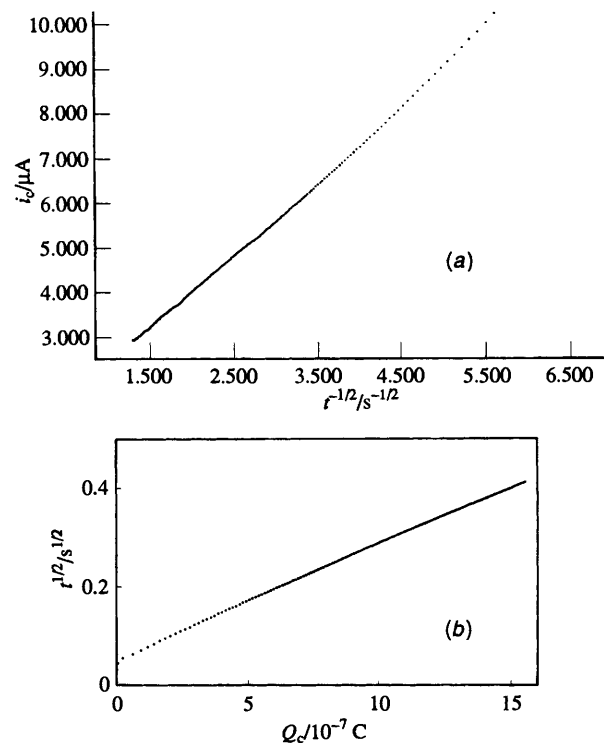


Fig. 2 Double step potential for 1.0 mmol dm<sup>-3</sup> catechol violet: (a)  $i_c$  vs.  $t^{1/2}$  relation, (b)  $t^{1/2}$  vs.  $Q_c$  relation

In the double step experiment, two potential steps are applied to the system. The electrolysis is performed in the first step at a potential where the rate of the electron-transfer product is controlled only by the diffusion of the starting material to the surface of the electrode. The potential is then switched back to the initial value after a pulse of duration time,  $\tau$ , and the resulting current decay is controlled by the diffusion of the chemically unreacted product. The experiments are performed by varying the switching duration time over a suitable range and comparing the results with the theoretical response ratio for various mechanisms in an attempt to find a satisfactory match.

**Behaviour at pH 1.8.** The electrode potential is stepped from 0.0 V (in which no Faradaic current flows) to  $-0.5$  V (sufficiently cathodic compared with the peak potential and the concentration of the depolarizer at the electrode surface is zero) where the cathodic current is determined solely by the diffusion of the starting depolarizer to the electrode surface. Then at some switching time,  $\tau$ , the potential is suddenly returned to the initial potential value of 0.0 V. The resulting anodic current, which is determined by the diffusion-controlled reoxidation of the reduced form produced during the switching time, gives a measure of the unreacted reduced form.

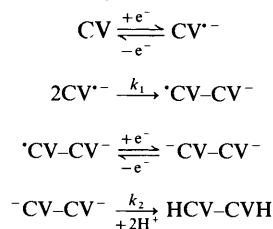
The cathodic chronoamperograms were analysed using eqn. (5). Plots of  $i_c$  versus  $t^{1/2}$  for each value of the switching time  $\tau$  were made. Straight lines are obtained with correlation coefficients of 0.999 for all duration times. Typical data are represented in Fig. 2. These results indicate that the initial reduction of catechol violet is a simple diffusion-controlled process over the entire range of time used. The diffusion coefficient of catechol violet is calculated from the slopes of the straight lines obtained and the average value is  $(4.83 \pm 0.29) \times 10^{-6}$  cm<sup>2</sup> s<sup>-1</sup>. The calculated value is consistent with the previously reported polarographic value for phenol red.<sup>2</sup>

According to eqn. (7) it is found that the charge,  $Q$ , correlates satisfactorily with the square root of time,  $t^{1/2}$  for all the switching times used ( $r = 0.9996$ , cf. Fig. 2). This strongly supports the chronoamperometric results that the cathodic response is diffusion-controlled. From the slopes of the straight

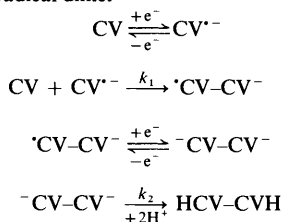
lines obtained the diffusion coefficient is calculated. The average value is in good agreement with the above obtained value and the literature value as well.

The analysis of the chronocoulograms involved the measure of the charge ratio,  $Q_R$ , for a series of switching times,  $\tau$ , by matching the  $Q_R$  vs.  $\log \tau$  curves with the theoretical working curves that had been calculated for the different electrode mechanisms by Hanafey *et al.*<sup>26</sup> These results are consistent with the initial hypothesis that the electrochemical reduction of catechol violet at lower pHs (1.8) proceed *via* ECEC mechanisms. Several mechanisms are considered for the ECEC kinetics as possible reaction pathways. These mechanisms are shown in Scheme 1, in which CV represents the  $H_3CV^-$  species.

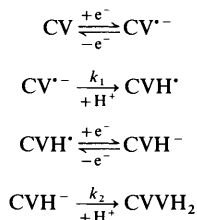
(a) ECEC, radical-radical dimer



(b) ECEC, parent-radical dimer



(c) ECEC, first order



Scheme 1

They include ECEC, the radical-radical dimer when  $k_2/k_1[A] = 0.05$ , ECEC, the parent-radical dimer when  $k_2/k_1[A] = 0.05$  and ECEC, first-order when  $k_2/k_1 = 0.1$ . Since the formed radical anion intermediate and the parent depolarizer are very bulky and sterically hindered species, it is reasonable to exclude the dimerization pathways [(a) and (b) mechanisms]. Thus, the ECEC, first-order mechanism is likely to be the pathway for electrochemical reduction of catechol violet. It is found that the experimental data obtained fit the theoretical working curve for this mechanism. Typical results for different values of  $\tau$  and the working curves for the possible mechanisms in Scheme 1 and disproportionation pathway are represented in Fig. 3, where the points are the experimental data and the lines represent the theoretical working curves for the suggested mechanisms. The best fit is clearly the ECEC, first-order mechanism in which the rate-determining step is the chemical reaction for the protonation of the anion to the final product with rate constant,  $k_2$ . The rate constant  $k_1$  is calculated as follows: for each value of charge ratio,  $Q_R$ , the value of the kinetic parameter,  $k_1\tau$ , is obtained from the working curve. The rate constant  $k_1$  is calculated directly from the slope of the plot of  $k_1\tau$  versus  $\tau$ . A good straight line which passes through the origin is obtained. A typical curve is shown in Fig. 3. The calculated rate constant  $k_1$  is  $12.04 \text{ s}^{-1}$ . The rate

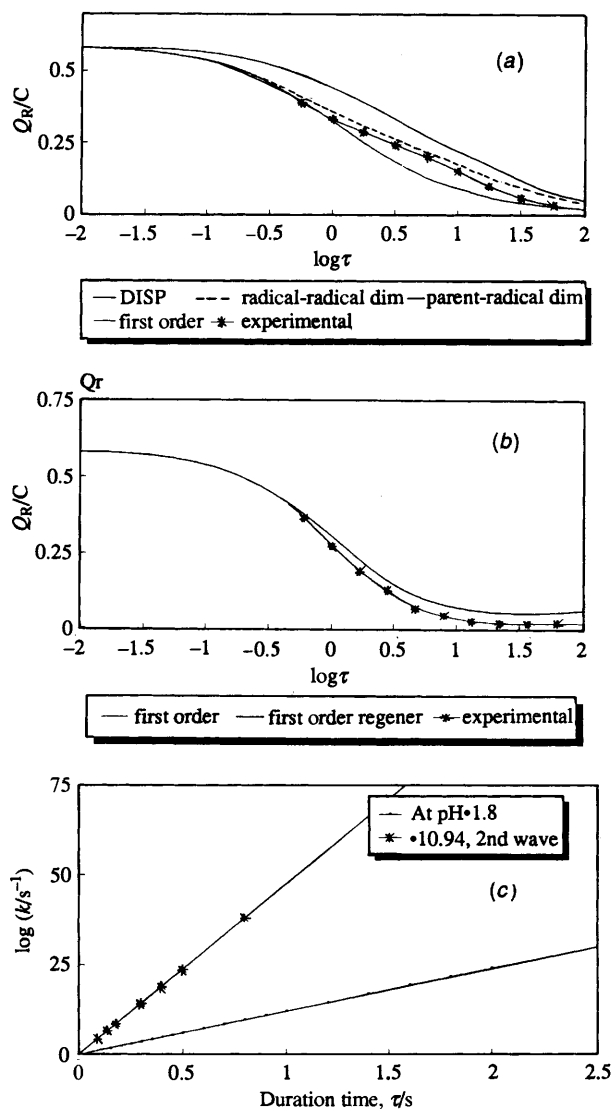


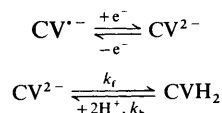
Fig. 3 Best fit of the chronocoulometric experimental data and the working curves for the possible reduction mechanisms of catechol violet: (a) pH 1.8, (b) pH 10.94, second wave, (c) relation between  $\log k$  and  $\tau$  at pH = 1.8 and 10.94 at second wave

constant  $k_2$  is calculated to be  $1.204 \text{ s}^{-1}$ . These findings strongly suggest the exclusion of the possibility of disproportionation of the neutral radical formed as was observed with other phenolsulfonephthaleins<sup>1,2,4</sup> in acid solutions. Note that the disproportionation mechanisms are excluded on the basis described above that the formed radical anion intermediate and the parent molecule are very bulky and sterically hindered species.

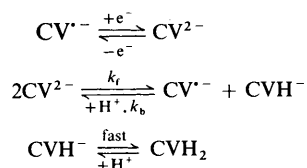
**Behaviour at pH 10.94.** In the double step studies at pH 10.94, the voltage is stepped from  $E_1$  to  $E_2$  to  $E_1$ , where  $E_1 = -0.75$  and  $E_2 = -1.0 \text{ V}$  for the second cv wave. With the aid of eqn. (5), the cathodic chronoamperometric responses were analysed. Linear least-square regression lines are obtained for the dependence of the cathodic current on  $t^{-1/2}$  with a correlation coefficient of 0.999 for each duration time used. Thus, the electrochemical reduction of catechol violet at pH 10.94 *via* the second cv wave is a diffusion-controlled process. The average diffusion coefficient is determined from these relations to be  $(4.68 \pm 0.1) \times 10^{-6} \text{ cm}^2 \text{ s}^{-1}$ . The estimated value is in good agreement with the value calculated above at lower pHs and the literature value.<sup>2</sup> On the other hand, analysis of the chronocoulograms according to eqn. (7), the diffusion-controlled nature of the process is confirmed ( $r = 0.999$ ) and the diffusion coefficient for the title compound is consistent with the above estimated value.

On fitting the experimental data, *i.e.* the charge ratio,  $Q_R$ , for a series of duration times with the theoretical working curves, it is seen that the experimental response matches the working curve for the EC mechanisms. The EC mechanisms considered as possible reaction pathways are represented in Scheme 2, in

(a) EC, first-order



(b) EC, first-order regeneration



Scheme 2

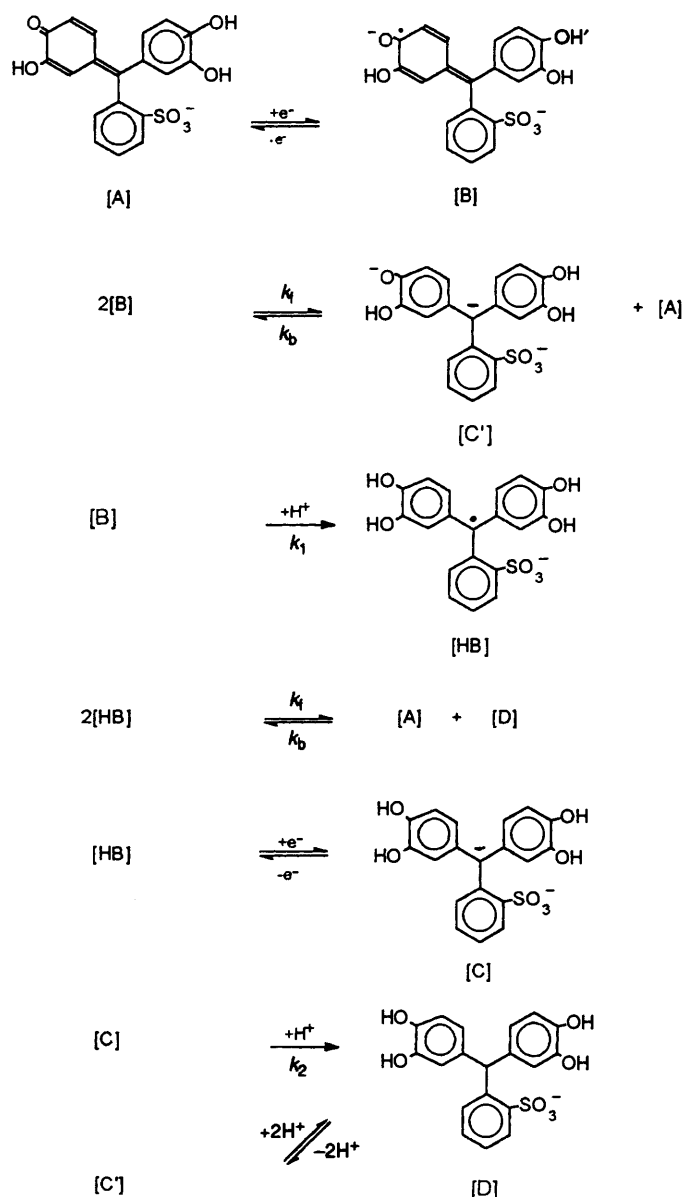
which CV represents the  $\text{HCV}^{3-}$  species. These mechanisms comprise EC, first-order at  $k_b/k_f = 0.01$ , and EC, first-order regeneration at  $k_b[\text{CV}]/k_f = 0.01$ . It is found that the experimental responses match correctly the theoretical working curve for the EC, first-order at  $k_b/k_f = 0.01$ . Thus, the electrochemical reduction of catechol violet at pH 10.94 in the potential range of the second cv wave is likely to proceed *via* the EC, first-order at  $k_b/k_f = 0.01$  pathway. Fig. 3 illustrates the fitting response along with the theoretical working curves for the possible pathways. The first-order rate constant  $k_f$  is determined following the above procedure. From the graph shown in Fig. 3, the values of  $k_f$  and  $k_b$  are calculated to be 47.4 and  $0.47 \text{ s}^{-1}$ , respectively.

### Digital simulation

**Behaviour at pH 1.8.** A scheme for the electrochemical reduction of catechol violet at pH 1.8 based on an ECEC, first-order and second-order disproportionation, is proposed and tested by digital simulation (*cf.* Scheme 3). Initial electron transfer to the catechol violet molecule, species A, results in formation of radical-anion, B. This redox couple is assigned to the standard potential,  $E_1^\circ$ . The radical anion, B will either (i) be protonated in the first-order step with a rate constant of  $k_1$  or in a fast reaction to form neutral radical, HB, or (ii) disproportionate in a second-order reaction<sup>1,2</sup> with rate constants of  $k_f$  and  $k_b$  to form the starting molecule A and the dianion C', which is protonated rapidly to the final product, D, following EC, second-order disproportionation kinetics.

The neutral radical, HB, can then undergo further electron transfer ( $E_2^\circ$ ) to form monoanion, C, which will yield the final product, D, *via* a first-order protonation process with rate parameter  $k_2$  following the ECEC, first-order mechanism. Alternatively, the neutral radical can disproportionate to the initial molecule, A, of the title compound and the final product, D, through a second-order process with rate constants  $k_f$  and  $k_b$  following EC, second-order disproportionation kinetics. As a result of the simulations when the disproportionation of the radical anion, B, or neutral radical, HB, is considered to be the pathway of the reduction, unsatisfactory fits are obtained.

To establish the theoretical working curves, digital simulation of the proposed mechanism was carried out. The heterogeneous electron transfer reactions are assumed to be rapid with a  $k^s$  value of  $1.0 \text{ cm}^{-1} \text{ s}^{-1}$  and  $\alpha = 0.5$  and diffusion coefficients for all species are identical. Shown in Fig. 1 is a simulation for the reduction of catechol violet at pH 1.8, the solid curve is the experimental voltammogram and the circles represent the simulation. With regard to the proposed mechanism shown in Scheme 3, two homogeneous kinetic

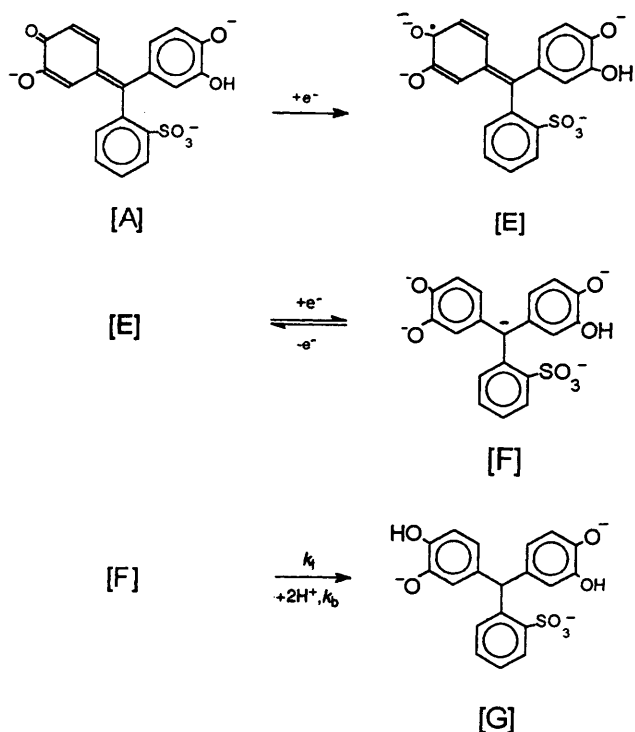


Scheme 3

processes are considered (if one ignores the DISP process), namely, the first-order protonation of radical anion, B, and of the monoanion, C, with respective rate constants  $k_1$  and  $k_2$ . When  $k_2$  is larger than  $k_1$  in the simulation, satisfactory fits are not obtained. (No reversibility is seen for the simulated cyclic voltammograms.) Setting  $k_2$  equal to  $k_1$  still causes no reversibility to appear in the simulated voltammogram. Only when  $k_2$  is smaller than  $k_1$  are satisfactory fits obtained as shown in Fig. 1. In this simulation  $k_1 = 12.04 \text{ s}^{-1}$  and  $k_2 = 1.2 \text{ s}^{-1}$ . It is interesting to compare this result with that obtained in the chronocoulometric results.

Values for  $\alpha$ ,  $k^s$  and  $E^\circ$  needed to obtain a best simulated fit are 0.31,  $6.8 \times 10^{-3} \text{ cm s}^{-1}$  and  $-0.425 \text{ V}$ , respectively for the first electron transfer and 0.55,  $0.153 \text{ cm s}^{-1}$  and  $-0.425 \text{ V}$  for the second electron transfer. Because the possibility exists that the species HB can be more easily reduced than the starting material A, the reduction mechanism shown in Scheme 3 must take the DISP reaction into account. However, if one includes the DISP reaction an unsatisfactory fit results. Thus, DISP processes have not been considered.

**Behaviour at pH 10.94.** For simulation of current-potential traces for the reduction of catechol violet at pH 10.94, Scheme 4 represents a mechanism that has consistently yielded the most satisfactory agreement with experimental results. Following the



chronocoulometric results, the present mechanism is based on the EEC kinetics in which the substrate, A, undergoes irreversible electron transfer ( $E_1^o$ ) to form radical anion, E, which then undergoes reversible electron transfer ( $E_2^o$ ) to give the dianion, F. Species F is then protonated through a first-order process to yield the final product, G with kinetic parameters, respectively,  $k_f$  and  $k_b$ .

In simulating the cyclic voltammograms shown in Fig. 1, one uses only the mechanistic steps illustrated in Scheme 4. For the first wave  $\alpha_1 = 0.40$ ,  $k_1^s = 5 \times 10^{-4} \text{ cm s}^{-1}$  and  $E_1^o = -0.590 \text{ V}$  and for the second wave  $\alpha_2 = 0.43$ ,  $k_2^s = 0.051 \text{ cm s}^{-1}$  and  $E_2^o = -0.95 \text{ V}$ . Values used for the first-order homogeneous kinetic parameters are  $k_f = 47.4$  and  $k_b = 0.5 \text{ s}^{-1}$ . Using these values the simulation agrees very well with the experimental voltammogram. It is interesting to note that for the reduction of catechol violet  $k_b$  is required to be larger than  $k_f$ .

## References

- 1 For Part I see R. Abdel-Hamid, *J. Electrochem. Soc. India*, 1985, **34**, 93.
- 2 J. K. Senne and L. M. Marple, *Anal. Chem.*, 1970, **42**, 1147.
- 3 P. J. Kadirka and R. S. Nicholson, *Anal. Chem.*, 1972, **44**, 1786.
- 4 M. M. Ghoneim, A. M. Khalil and A. M. Hassanein, *Electrochim. Acta*, 1979, **21**, 623.
- 5 M. Yeber and L. J. Csany, *J. Electroanal. Chem.*, 1979, **101**, 419.
- 6 M. M. Ghoneim, R. M. Issa and R. A. Mahmoud, *Monatsh. Chem.*, 1981, **112**, 293.
- 7 W. D. Wakley and L. P. Varga, *Anal. Chem.*, 1972, **44**, 169.
- 8 S. Raheem and K. M. M. K. Prasad, *Talanta*, 1993, **40**, 1809.
- 9 K. M. M. K. Prasad and S. Raheem, *Microchim. Acta*, 1993, **112**, 63.
- 10 J. R. Kramer, J. Gleed and K. Gracey, *Anal. Chim. Acta*, 1994, **284**, 599.
- 11 K. M. M. K. Prasad, P. Vijayalekshmi and C. K. Sastri, *Analyst*, 1994, **119**, 2817.
- 12 J. Kobayashi, M. Baba and M. Miyazaki, *Anal. Sci.*, 1994, **10**, 287.
- 13 B. Fairman, A. Sanzmedel, M. Gallego, M. J. Quintela, P. Jones and R. Benson, *Anal. Chim. Acta*, 1994, **286**, 481.
- 14 D. J. Hawke and H. K. J. Powell, *Anal. Chim. Acta*, 1994, **299**, 257.
- 15 L. F. Capitanvallvey, M. C. Valencia and G. Miron, *Anal. Chim. Acta*, 1994, **289**, 365.
- 16 D. V. Vukomanovic and G. W. Vanloon, *Fresenius J. Anal. Chem.*, 1994, **350**, 352.
- 17 R. B. Zhn, J. L. Han and H. Y. Chen, *Chem. J. Chinese Univ-Chin.*, 1995, **16**, 35.
- 18 R. S. Nicholson and I. Shain, *Anal. Chem.*, 1964, **36**, 706; 1965, **37**, 178, 190.
- 19 R. S. Nicholson, *Anal. Chem.*, 1965, **37**, 1351.
- 20 R. S. Nicholson, *Anal. Chem.*, 1966, **38**, 406.
- 21 S. W. Feldberg, in *Electroanalytical Chemistry*, ed. A. Bard, Marcel Dekker, New York, 1969, vol. 3.
- 22 S. D. Nadler, J. G. Dick and C. H. Langford, *Can. J. Chem.*, 1985, **63**, 2732.
- 23 D. K. Gosser, Jr. and F. Zheng, *Talanta*, 1991, **38**, 715.
- 24 P. He and L. R. Faulkner, *Anal. Chem.*, 1986, **58**, 517.
- 25 J. C. K. Placeres, M. T. S. Alacios and F. J. G. Montelongo, *Talanta*, 1992, **39**, 649.
- 26 M. K. Hanafey, R. L. Scott, T. H. Ridgway and C. N. Reilly, *Anal. Chem.*, 1978, **50**, 116.

Paper 5/04733A

Received 18th July 1995

Accepted 31st October 1995